Comparison of Radar-Based Human Detection Techniques

Sevgi Zübeyde Gürbüz[1], William L. Melvin[2], and Douglas B. Williams[1]

[1]School of Electrical and Computer Engineering
[2]Georgia Tech Research Institute
Georgia Institute of Technology, Atlanta, GA

***Abstract* - Radar offers unique advantages over other sensors in the human detection problem, such as remote operation during virtually all weather and lighting conditions. Many radar-based human detection systems today employ Fourier analysis, such as spectrograms. However, spectrograms perform poorly in high clutter environments. Also, an inherent SNR loss is caused by the implicit assumption of linear target phase. In this paper, human modeling is used to derive a more accurate non-linear approximation to the true non-linear target phase and the liklihood ratio is optimized over unknown parameters to enhance detection performance. Performance is compared both analytically and through MATLAB simulations.**

I. INTRODUCTION

Much of the current research in human detection is focused on the application of Fourier transform based techniques, such as spectrogram analysis. In 2002, Geisheimer [1] experimentally showed that a measured human spectrogram could be obtained by summing the spectrograms obtain from the reflections off each individual body part. This result was theoretically confirmed by Van Dorp [2], who based his calculations on a kinematic walking model developed by Thalmann [3]. Comparisons between the human spectrogram and the spectrograms of other animals, such as dogs, showed that certain characteristics were unique to just humans and that these characteristics could be used in human detection and identification. For example, Otero [4] proposed techniques based on features extracted from the spectrogram to differentiate humans from dogs, or even women from men. Greneker [5] designed and tested a suicide bomber detection system based on variations in the spectrogram caused by the presence of a bomb.

However, all of these systems were used in close proximity or in situations where the clutter was minimal. In practice, spectrograms are almost completely obscured in high clutter environments, rendering impossible the accurate extraction of any information [6]. Furthermore, application of the FFT implicitly assumes that the target phase history is linear, an assumption not generally true for non-linear phase human targets. The resulting phase mismatch results in an inherent SNR loss due to the detector, decreasing even further the chances of detecting slow-moving human targets.

In this paper, Thalmann's kinematic model is used as a basis for deriving a more accurate non-linear approximation to the true target phase. Maximum liklihood estimates (MLE) of unknown geometry and target parameters are obtained to maximize the likelihood ratio and resulting matched filter output. The performance of the FFT-based matched filter is compared to that of the proposed optimized linear and nonlinear phase detectors, as well as to the ideal "clairvoyant" detector, representing the best performance attainable with complete knowledge of the target.

II. SIGNAL MODELLING

In general the received radar signal is comprised of the sum of noise plus a time-delayed and phase-shifted version of the transmitted chirp signal. For the purposes of this paper, the noise is modeled as being complex Gaussian. Then the target return may be expressed as

$$s_r(n,t) = a_t rect\left(\frac{\hat{t}-t_d}{\tau}\right) e^{j\left[-2\pi f_c t_d + \pi\gamma(\hat{t}-t_d)^2\right]}, \qquad (1)$$

where a_t is the amplitude as given by the radar range equation; $t_d \equiv 2R/c$; R is the range from the antenna to target; c is the speed of light; τ is the pulse width; γ is the chirp slope; f_c is the transmitted center frequency; and n is the pulse number.

If the noise is small compared to the signal energy, the peak of the pulse compression output occurs at the range bin in which the target is present:

$$y_p[n] = a_t \tau e^{-j2\pi f_c t_d} = \frac{A}{R^2[n]} e^{-j\frac{4\pi f_c}{c}R[n]}, \qquad (2)$$

where A is an unknown amplitude parameter and the slow-time dependence on pulse number, n, is emphasized with brackets. Typically this peak is indiscernable in noise, so that the detection test must be

applied separately over each range bin. However, in the case of human targets, the center of the range bin, r_b, is not a sufficiently accurate approximation to the true target location. Most human target motion will generally remain within one range bin, excepting the case of very long dwell times.

A better approximation of target range may be obtained by assuming that the motion is linear along a constant angle, θ, relative to the initial antenna-target vector (see Fig. 1). First define $\mathbf{r_1}$ as the vector between the aperture and initial target location; $\mathbf{r_n}$ as the vector between the aperture and target location at the n^{th} pulse; and $\mathbf{h}$ as the vector describing human motion. Then,

$$|\mathbf{r_n}|^2 = |\mathbf{r_1}|^2 + |\mathbf{h}|^2 - 2|\mathbf{r_1}||\mathbf{h}|\cos\theta \tag{3}$$

Since $|\mathbf{h}| << |\mathbf{r_1}|$ and $\sqrt{1+x} \approx 1 + x/2$ for small x,

$$|\mathbf{r_n}| \approx |\mathbf{r_1}| - |\mathbf{h}|\cos\theta \tag{4}$$

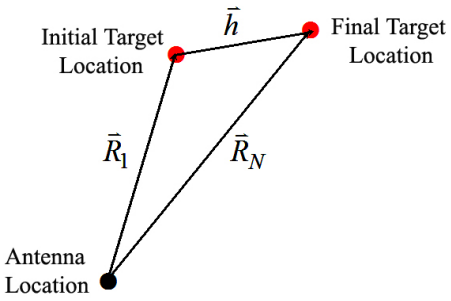

Figure 1. Target Geometry

A. *Linear Phase Approximation*

If we model $|\mathbf{h}|$ as simply a constant velocity, v, times the pulse repetition interval, T, times the pulse number, n, then subsituting (4) into (2) results in a linear phase model

$$y_p[n] \approx \frac{A}{r_b^2} e^{-j\frac{4\pi f_c}{c}(r - nTv\cos\theta)}, \tag{5}$$

where the range term of the amplitude has been modeled as r_b since the effect of perturbations in the amplitude is negligible; and $|\mathbf{r_1}|=r$, an unknown parameter.

B. *Non-Linear Phase Approximation*

The Thalmann kinematic model for human walking consists of a set of equations that describe the time varying position and change in angle of key joints and limbs. Combined, they can be used to calculate the time-varying position of any point in the human body. In this work, the human body has been divided into twelve parts: head, torso, two upper arms, two lower arms, two thighs, two lower legs and two feet. Each body part is modeled as a point target with a cylindrical radar cross section (RCS), excepting the head which is modeled with a spherical RCS. The total radar return is given by the sum of the returns from each point target.

Each kinematic equation depends on two variables: 1) RV, the ratio of velocity (v) to thigh height (HT), and 2) t%, a time index taken relative to the beginning of a step. Mathematically,

$$RV = \frac{v}{HT} \tag{6}$$

and

$$t\% = \frac{nT}{1.346}\sqrt{RV} + t_0 \tag{7}$$

where t_0 is a constant indicating the point within the stepping cycle that the first transmitted pulse reflects from the target. The velocity profile of each body part can be clearly seen in the resulting human spectrogram. The strongest return results from the low-amplitude sinusoidal motion of the torso, while the largest Doppler amplitude is given by the trajectory of the feet. A typical measured spectrogram can be visually matched to a sample simulated spectrogram, as shown in Fig. 2.

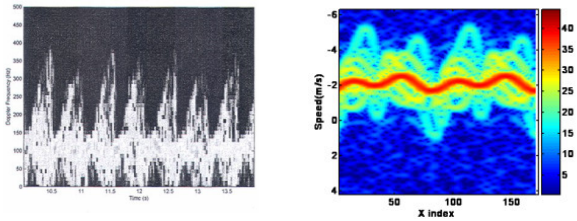

(a) (b)

Figure 2. Human spectrograms: (a) Measured (from [4]) (b) Simulated.

Because of the strong signal strength of the return from the torso, only the torso equations of motion will be used in calculating $|\mathbf{h}|$:

$$|\mathbf{h}|^2 = OS_V^2 + OS_L^2 + OS_{FB}^2 \tag{8}$$

where

$$OS_V = 0.015RV\left[-1 + \sin(4\pi t\% - 0.7\pi)\right]$$
$$OS_L = A_L \sin(2\pi t\% - 0.2\pi)$$
$$A_L = \begin{cases} -0.032 & \text{for } 0.5 < RV < 2.3 \\ -0.128RV^2 + 0.128 & \text{for } RV < 0.5 \end{cases}$$

and

$$OS_{FB} = A_a \sin(4\pi\% + 2\phi_a)$$

$$A_a = \begin{cases} -0.021 & \text{for } 0.5 < RV < 2.3 \\ -0.084RV^2 \_ 0.084RV & \text{for } RV < 0.5 \end{cases}$$

$$\phi_a = -0.127 + 0.731\sqrt{RV}$$

The torso model can be further simplified by neglecting the case when RV < 0.5, as most human targets will not fall in that range and by then averaging the trajectories for 0.6 < RV < 2.3, the maximum RV for which Thalmann's model is defined. The individual torso trajectories and resulting average trajectory is shown in Fig. 3.

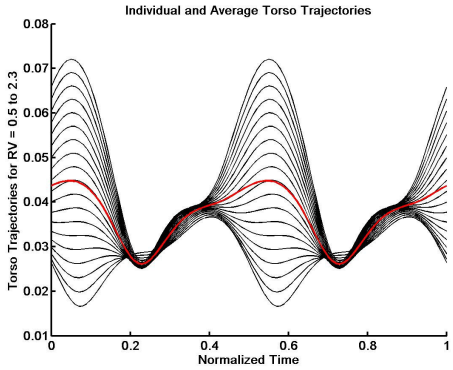

Figure 3. Individual and Averaged Torso Trajectories.

A sinusoidal curve fit to the average torso trajectory may be then found to be

$$|\mathbf{h}| = h[n] \approx 0.0108\cos\left(\frac{4\pi T}{1.346}\sqrt{RV}\,n + \phi\right) + 0.037 \qquad (9)$$

where RV and ϕ are unknown parameters. This expression may be substituted into (2) and (4) to obtain

$$y_p[n] \approx \frac{A}{r_b^2} e^{-j\frac{4\pi f_c}{c}(r - h[n]\cos\theta)} \qquad (10)$$

III. DETECTOR DESIGN

The detector must make a decision between two hypotheses:

$$H_0: \quad \mathbf{x} = \mathbf{w}$$
$$H_1: \quad \mathbf{x} = \mathbf{y_p} + \mathbf{w}$$

where **w** is Gaussian noise with covariance matrix $\mathbf{R_I}$ and $\mathbf{y_p}$=y_p[n] is the true target signal. As it is not possible to know apriori the interference covariance matrix, instead an estimate is used, $\hat{\mathbf{R}}_\mathbf{I} = E[\mathbf{x_{H0}}\mathbf{x_{H0}^H}]$. Similarly, the true target signal is approximated with an estimate, $\hat{\mathbf{y}}_\mathbf{p}$, which will change depending on whether we apply an FFT, or a linear or nonlinear approximation to |**h**|.

Assuming that we've obtained a suitable model for the expected target return, a likelihood ratio test may be formed to determine the detector decision rule.

$$p(\mathbf{x}; H_0) = \frac{1}{\pi^N \left\|\hat{\mathbf{R}}_\mathbf{I}\right\|} e^{-\mathbf{x}^H \mathbf{R}_\mathbf{I}^{-1}\mathbf{x}}$$
$$p(\mathbf{x}; H_1) = \frac{1}{\pi^N \left\|\hat{\mathbf{R}}_\mathbf{I}\right\|} e^{-(\mathbf{x}-\hat{\mathbf{y}}_\mathbf{p})^H \mathbf{R}_\mathbf{I}^{-1}(\mathbf{x}-\hat{\mathbf{y}}_\mathbf{p})} \qquad (11)$$
$$\text{Decide } H_1 \text{ if } \frac{p(\mathbf{x}; H_1)}{p(\mathbf{x}; H_0)} > \gamma \rightarrow \text{Re}\left\{\hat{\mathbf{y}}_\mathbf{p}^\mathbf{H}\mathbf{R}_\mathbf{I}^{-1}\mathbf{x}\right\} > \gamma'$$

where $\gamma' = \sqrt{\text{Re}\{\hat{\mathbf{y}}_\mathbf{p}^\mathbf{H}\mathbf{R}_\mathbf{I}^{-1}\mathbf{y}_\mathbf{p}\}} \cdot Q^{-1}(P_{FA})$ and P_{FA} is the desired probability of false alarm.

A. FFT-Based Detector

Taking the FFT across-slow time for each range bin yields the following estimate to the true target signal:

$$\hat{y}_{p,fft}[n] = \frac{|Y_p(f_{peak})|}{N/2}\sqrt{2} \cdot e^{-j2\pi f_{peak}^c Tn} \qquad (12)$$

B. Optimized Linear Phase (OLP) Detector

Inspection of (5) reveals three unknown parameters over which the likelihood ratio must be maximized: A, r, and $v_r \equiv v\cos\theta$. If we express $\mathbf{y_p}$=A**s**, the an MLE estimate of A may be found as

$$\hat{A} = \frac{\text{Re}\{\mathbf{s^H x}\}}{\mathbf{s^H s}} \qquad (13)$$

The unknown parameters in the phase may be estimated from the tangent of the phase, found by taking the ratio of the imaginary and real parts of the signal. This operation will convert the complex Gaussian noise **w** into Cauchy noise with distribution

$$p(x; \mu, \gamma) = \frac{1}{\pi\gamma\left[1 + \left(\frac{x-\mu}{\gamma}\right)^2\right]} \qquad (14)$$

Here, μ is a location parameter for the Cauchy distribution that is y_p under H_1 and zero under H_0. The parameter γ is an unknown constant that drops out during maximization.

The MLE estimates of r and v_r can be shown to be found by solving the following equation, where the derivative is taken with respect to r or v_r, depending on which estimate is being computed:

$$\sum_{n=1}^{N}\left(x[n] - \frac{\text{Im}\{\hat{y}_p[n]\}}{\text{Re}\{\hat{y}_p[n]\}}\right)\left(\frac{\text{Im}\{\hat{y}_p[n]\}}{\text{Re}\{\hat{y}_p[n]\}}\right)' = 0 \qquad (15)$$

The resulting set of three equations with three unknowns is highly nonlinear, making impossible a closed form expression for the MLE estimates. However, these equations may be numerically solved in MATLAB to derive a numerical solution for the estimates. When the MLE estimates $\hat{A}, \hat{r}, \text{and } \hat{v}_r$ are substituted into (5) and used in (11), the OPT detector is obtained.

C. Optimized Non-Linear Phase (ONLP) Detector

The same procedure as outlined in the previous section is employed to derive the MLE estimates for the optimized non-linear phase detector based on the nonlinear motion approximation expressed in (9). With the Thalmann-based expression for h, (15) is numerically solved in MATLAB to obtain MLE estimates for the unknown parameters A, r, VR, ϕ, and θ. Substitution of these estimates into (10) and (11) yield the ONLP detector.

D. Clairvoyant Detector

Naturally the best possible performance is obtained if we have sufficient information to identically know the true signal embedded in noise, $\mathbf{y_p}$. Thus, the optimal clairvoyant detector is obtained by using $\hat{\mathbf{y}}_\mathbf{p} = \mathbf{y_p}$ in (11).

IV. PERFORMANCE

Detector performance is compared both analytically and via simulations in MATLAB. The expected receiver operating characteristic (ROC) curves may be mathematically written as

$$P_D = Q\left\{Q^{-1}(P_{FA}) - \sqrt{\mathrm{Re}\{\hat{\mathbf{y}}_\mathbf{p}^\mathbf{H}\mathbf{R}_\mathbf{I}^{-1}\mathbf{y_p}\}}\right\} \qquad (16)$$

Simulations were conducted for a human target walking at 2 m/s approximately 7 km away from a radar antenna with a transmitter power of 1.8 kW, center frequency of 1 GHz, and a dwell time of 100 ms.

For this example, the estimates of the phase of y_p are compared in Fig. 4. Notice that the nonlinear phase approximation closely follows the true target phase.

Theoretical and simulated P_D versus P_{FA} and P_D versus SNR curves are shown in Figs. 5, 6, 7 and 8. As expected, the nonlinear phase detector outperforms all other detectors, performing just under the ideal clairvoyant detector. At an SNR of -20 dB, the ONLP detector has a P_D that is roughly five times higher than that of the FFT-based detector. The SNR loss for the ONLP detector is 4 dB less than that of the FFT-based detector for most P_Ds. The OLP detector also performs much better than the FFT-based detector, although still falling short of the ONLP detector.

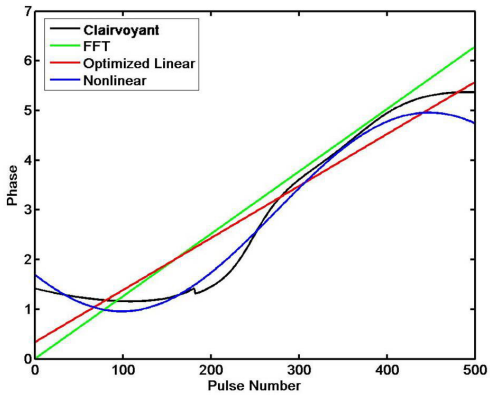

Figure 4. Approximated and True Signal Phase Histories

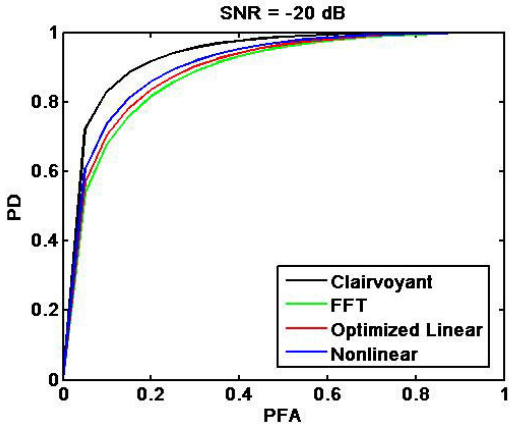

Figure 5. Theoretical ROC Curves for All Detectors at a SNR of -20 dB

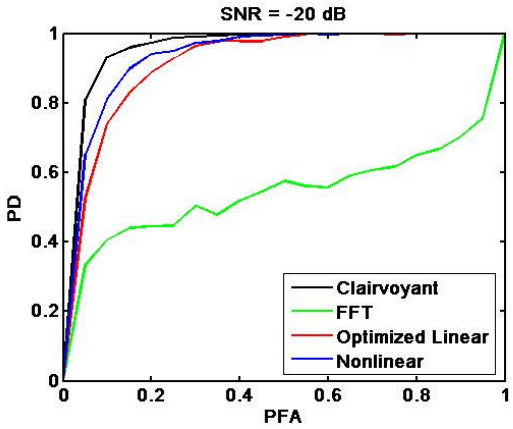

Figure 6. Simulated ROC Curves for All Detectors at an SNR of -20 dB

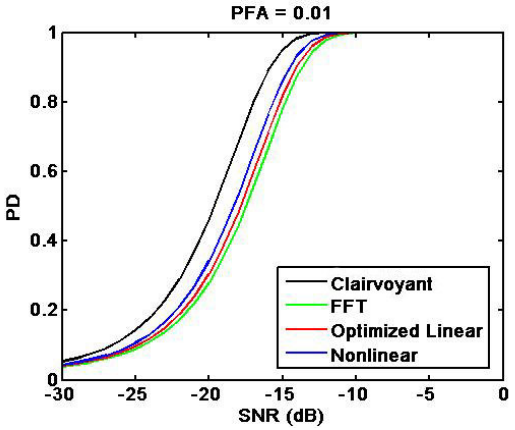

Figure 7. Theoretical Probability of Detection versus SNR at a 1% False Alarm Rate for All Detectors

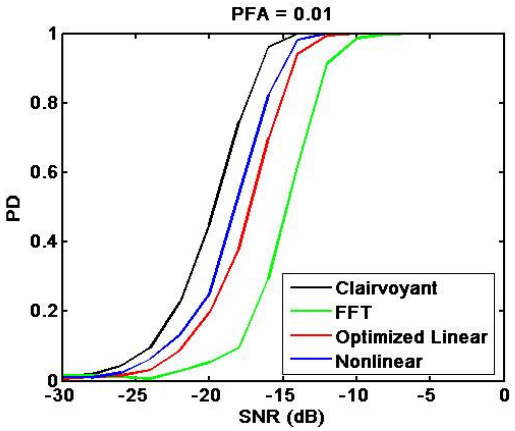

Figure 8. Simulated Probability of Detection versus SNR at a 1% False Alarm Rate for All Detectors

V. CONCLUSIONS

A new human target detector design is presented based on more accurate modeling of the true target phase history and optimization of the likelihood ratio test is presented. Theoretical analysis and MATLAB simulations of performance show that the new detector achieves substantially higher detection probabilities over a range of SNRs relative to the currently obiqutous FFT-based detector.

ACKNOWLEDGEMENT

This work is supported by the U.S. Air Force Research Laboratory, Sensors Directorate, under contract FA8650-05-D-1912 and public release approval #RY-07-0461. The views and conclusions contained in this document are those of the authors and should not be interpreted as representing the official policies, either expressed or implied, of the U.S. Government.

VI. REFERENCES

[1] Geisheimer, J.L., Greneker, E.F., and Marshall, W.S., ``A high-resolution doppler model of human gait'', in *Proc. of SPIE,* Vol. 4744, 2002.

[2] Van Dorp, P., and Groen, F.C.A., ``Human walking estimation with radar'', *IEE Proc. on Radar, Sonar and Nav.*, 150(5):356-365, 2003.

[3] Boulic, R., Thalmann, M.N., and Thalmann, D., ``A global walking model with real-time kinematic personification'', *Vis. Comput.,* 6:344-358, 1990.

[4] Otero, M., ``Application of a continuous wave radar for human gait recognition'', in *Proc. of SPIE*, Vol. 5809, pp. 538-548, 2005.

[5] Greneker, G., ``Very low cost stand-off suicide bomber detection system using human gait analysis to screen potential bomb carrying individuals'', in *Proc. of SPIE*, Vol. 5788, 2005.

[6] Gurbuz, S.Z., Melvin, W.L, and Williams, D.B. “Detection and Identification of Human Targets in Radar Data,” in *Proc. of SPIE Defense and Security Symposium*, April 9-13, Orlando, FL, 2007.